Journal of Engineering Mathematics **43:** 347–366, 2002.

Mathematical modelling of moisture-induced panel deformation

W. R. SMITH[1] and H. J. J. GRAMBERG
Department of Mathematics and Computing Science, Technische Universiteit Eindhoven, PO Box 513, 5600 MB Eindhoven, The Netherlands

Received 22 June 2001; accepted in revised form 16 April 2002

Abstract. A new mathematical model is introduced to describe the moisture-induced deformation in an elastic panel. The problem for the stresses is found to be singularly perturbed in the aspect ratio squared, the domain being split into four asymptotic regions. Determination of the matching constants is made possible by the introduction of a stress function in the boundary layer. Explicit expressions are derived for the stress and deformation in the three-dimensional problem. The predictions for deformation are compared with experimental results; the agreement is reasonable. The moment of the moisture concentration is found to be the crucial factor in determining panel warp. A model, which consists of two coupled parabolic equations, is also proposed for moisture transport in exterior applications. The disparate time-scales allow the system to be reduced to a single partial differential equation. In one parameter régime, a multiple-scale analysis further reduces this partial differential equation to an averaged equation which only requires solution over the long moisture-diffusion time-scale.

Key words: asymptotics, moisture transport, panel deformation

1. Introduction

The absorption of moisture may cause undesirable deformation in various situations (see, for example, [1]). Table tops are often constructed from cured phenol/formaldehyde resin reinforced with wood or cellulose fibres. Other applications include exterior wall coverings. The high natural fibre content makes such panels susceptible to deformation as a result of moisture variations. In this paper, we investigate the deformation of an elastic panel containing wood fibres, such as a table top.

Three modes of deformation are illustrated in Figure 1. If the relative humidity is uniform, then either swelling or shrinkage takes place, depending on whether the relative humidity is below or above a reference value. However, if the relative humidity is asymmetric, then warpage is observed. The moisture-induced swelling of a panel is analogous to the temperature-induced swelling in thermoelasticity [2], the model being very similar. However, there are two important differences, (i) the swelling due to moisture is not necessarily isotropic (although we will assume any anisotropy in the elastic properties to be negligible) and (ii) the time-scale to reach the steady state of the heat equation is typically less than a second, whereas the diffusion of moisture may take years (see below). The question of how asymmetries in the concentration of moisture influence the deformation is therefore of great significance.

The panel is assumed to have two planes of symmetry. Therefore, we will only study a quarter of the panel and apply the appropriate conditions on the planes of symmetry (see Figure 2). The lateral directions (length and width) are denoted by x and y, the transverse

[1]current address School of Mathematics and Statistics, The University of Birmingham, Edgbaston, Birmingham, B15 2TT, UK.

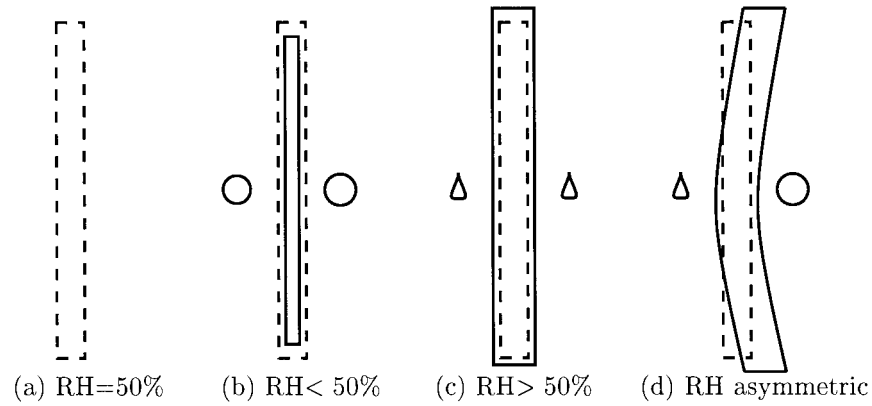

Figure 1. A schematic representation of the modes of deformation. The dashed (solid) lines are the perimeter of the panel before (after) deformation. The circles denote low relative humidity and the droplets high relative humidity. The modes are (a) no deformation, (b) shrinkage, (c) swelling and (d) warpage.

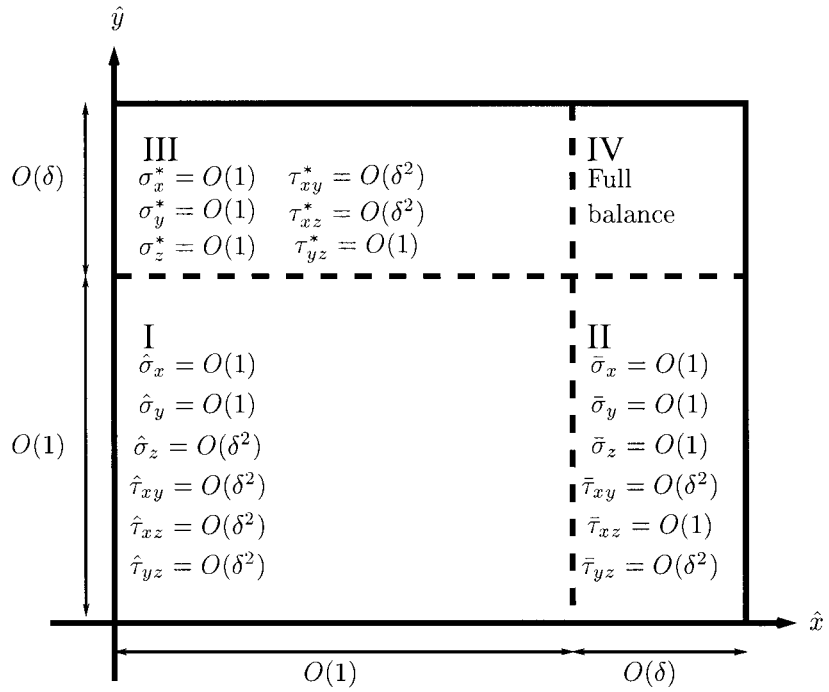

Figure 2. Two-dimensional representation of a symmetric panel with dimensionless variables. The length and width are denoted by $\hat{x}$ and $\hat{y}$ and the thickness by $\hat{z}$ (pointing out of the page). The panel is in the region $-1 < \hat{x} < 1$, $-W/L < \hat{y} < W/L$ and $-1 < \hat{z} < 1$ before deformation. The four asymptotic regions are labelled I to IV. Regions II, III and IV are much smaller than region I as $\delta \ll 1$.

direction (thickness) by z, the normal stresses by σ_x, σ_y and σ_z and the shear stresses by τ_{xy}, τ_{xz} and τ_{yz}. In classical thin-plate theory, the stress components σ_z, τ_{xz} and τ_{yz} are taken to be zero throughout the panel (see [3] and references therein). More recent approaches have assumed that $\sigma_z = 0$ throughout the panel [4]. We do not make any such assumptions. Our approach is based on the fullest leading-order balance in the asymptotic limit of small aspect ratio. Classical thin-plate theory also applies edge boundary conditions in terms of the average

Table 1. Physical data for a panel containing wood fibres

Symbol	Definition	Value
ρ	density	3×10^3 kg m $^{-3}$
c_p	specific heat capacity	2×10^3 J kg^{-1} K $^{-1}$
k	thermal conductivity	0·3 J s^{-1} m^{-1} K $^{-1}$
E	modulus of elasticity	10^{10} N m^{-2}
D	diffusion coefficient	8×10^{-13} m^{2}s^{-1}
L	half x-length	1 m
W	half y-length	1 m
h	half z-length	$1{\cdot}3 \times 10^{-2}$ m

displacements or of the stress and moment resultants. In this paper, we adopt a pointwise specification of stress at the boundary (see, for example, [5]).

We also take advantage of the aspect ratio to simplify the models for diffusion of moisture and conduction of heat. The lateral diffusion and conduction terms in the governing parabolic partial differential equation are smaller than the transverse diffusion and conduction terms by a factor of the aspect ratio squared. If the boundary conditions are independent of the lateral coordinates, then, apart from in the neighbourhood of the lateral boundaries, the leading-order concentration and temperature are only functions of the transverse direction and time. Throughout the paper we will adopt the assumption that the concentration and temperature are only functions of the transverse direction and time.

In interior applications, the two physical time-scales are associated with the diffusion of moisture through the panel and the elastic deformation; the former is given by $h^2/D \sim 4$ years and the latter by $h\sqrt{\rho/E} \sim 10^{-6}$s (where the parameters are given in Table 1). Panels are typically inspected a few days after being manufactured and we are particularly interested in explaining any warp which may have taken place over this time-scale. The time-scale for elastic deformations is so short that we will only retain time derivatives for the diffusion of the moisture. In exterior applications, the four physical time-scales are the two mentioned above for interior applications, the time-scale of a day over which the temperature and moisture uptake are periodic at leading order and the thermal conduction time-scale ($\rho c_p h^2/k \sim 300$s).

The purpose of this paper is to gain a better understanding of the process of panel deformation. We derive explicit expressions for the stress and deformation in the three-dimensional problem. One eventual aim is to minimise the warp, which is defined as the deflection of the centre plane ($z = 0$) in the transverse direction. The warp depends on the panel characteristics and moisture distribution. In exterior applications, swelling and shrinkage are the primary problems and here it is important to develop a model for the moisture transport.

The contents of the paper will now be outlined. Based on the above assumptions, a new mathematical model is introduced in Section 2. We choose to formulate the model in terms of stresses; this approach proving more amenable to our analysis. In Section 3, the model is non-dimensionalised enabling the dominant balances to be identified. The stresses are singularly perturbed in the aspect ratio squared with an outer expansion and three boundary-layer expansions. A solution is obtained in the boundary layer by introduction of a stress function. This stress function reduces the solution of six partial differential equations in four unknowns

to the solution of a single partial differential equation. The matching constants may then be determined. The displacements are deduced from the stresses. A new mathematical model for moisture transport in exterior applications, which consists of two parabolic equations for moisture diffusion and thermal conduction, is introduced in Section 4. The disparate time-scales allow the leading-order temperature to be expressed as the solution of a linear ordinary differential equation, an analytical solution being easily determined. In general, the moisture diffusion equation requires a numerical solution. However, in one parameter régime, a multiple-scale analysis reduces this problem to a partial differential equation over the long moisture-diffusion time-scale; the daily temperature variations are taken into account by an effective diffusion coefficient. In Section 5, the predictions for displacement are compared with experimental results over the time period of a few days. An example of moisture diffusion in an exterior application is also presented. Finally, Section 6 gives a brief discussion of the results.

2. Problem formulation

We define the deformation tensor as follows (see, for example, [2])

$$e_{ij} = \frac{1}{2}\left(\frac{\partial u_i}{\partial x_j} + \frac{\partial u_j}{\partial x_i}\right), \qquad i, j = 1, 2, 3,$$

where $u_1 = u$, $u_2 = v$ and $u_3 = w$ are the displacements and $x_1 = x$, $x_2 = y$ and $x_3 = z$. The deformation tensor is assumed to be split up into a part which represents the deformation caused by elastic effects and a part that represents the deformation caused by expansion of the material due to swelling, namely

$$e_{ij} = e_{ij}^{(el)} + e_{ij}^{(sw)}.$$

We assume that the deformation of the panel due to humidity is linearly dependent on the concentration of moisture inside the material. Experiments support this assumption (see Subsection 5.1.1). This leads to the the following set of equations for $e_{ij}^{(sw)}$

$$e_{11}^{(sw)} = \alpha_x c, \quad e_{22}^{(sw)} = \alpha_y c, \quad e_{33}^{(sw)} = \alpha_z c, \quad e_{12}^{(sw)} = 0, \quad e_{13}^{(sw)} = 0, \quad e_{23}^{(sw)} = 0,$$

where $c(z, t)$ is the concentration of moisture (in this section time t is viewed as a parameter), α_x, α_y and α_z represent the swelling in the x, y and z directions, respectively. Experiments predict that $\alpha_x/\alpha_z = \alpha_y/\alpha_z < 1$. We note that this model is analogous to thermoelasticity, except that in this case the strain due to moisture is anisotropic. We apply Hooke's Law to relate the deformation tensor to the stress tensor, to obtain

$$\begin{aligned} &\frac{\partial u}{\partial x} = \frac{((1+\nu)\sigma_x - \nu\Theta)}{E} + \alpha_x c(z,t), \frac{\partial v}{\partial y} = \frac{\big((1+\nu)\sigma_y - \nu\Theta\big)}{E} + \alpha_y c(z,t), \\ &\frac{\partial w}{\partial z} = \frac{((1+\nu)\sigma_z - \nu\Theta)}{E} + \alpha_z c(z,t), \end{aligned} \tag{1}$$

$$\begin{aligned} &\tau_{xy} = \frac{E}{2(1+\nu)}\left(\frac{\partial u}{\partial y} + \frac{\partial v}{\partial x}\right), \quad \tau_{xz} = \frac{E}{2(1+\nu)}\left(\frac{\partial u}{\partial z} + \frac{\partial w}{\partial x}\right), \\ &\tau_{yz} = \frac{E}{2(1+\nu)}\left(\frac{\partial v}{\partial z} + \frac{\partial w}{\partial y}\right), \end{aligned} \tag{2}$$

where $\Theta = \sigma_x + \sigma_y + \sigma_z$, E is the (constant) modulus of elasticity and ν is (constant) Poisson's ratio.

The three equations for conservation of momentum are

$$\frac{\partial \sigma_x}{\partial x} + \frac{\partial \tau_{xy}}{\partial y} + \frac{\partial \tau_{xz}}{\partial z} = 0, \quad \frac{\partial \tau_{xy}}{\partial x} + \frac{\partial \sigma_y}{\partial y} + \frac{\partial \tau_{yz}}{\partial z} = 0, \quad \frac{\partial \tau_{xz}}{\partial x} + \frac{\partial \tau_{yz}}{\partial y} + \frac{\partial \sigma_z}{\partial z} = 0. \tag{3}$$

The six compatibility conditions are

$$(1+\nu)\nabla^2\sigma_x + \frac{\partial^2\Theta}{\partial x^2} = -\frac{(\alpha_x + \nu\alpha_y)E}{(1-\nu)}\frac{\partial^2 c}{\partial z^2}, \tag{4}$$

$$(1+\nu)\nabla^2\sigma_y + \frac{\partial^2\Theta}{\partial y^2} = -\frac{(\alpha_y + \nu\alpha_x)E}{(1-\nu)}\frac{\partial^2 c}{\partial z^2}, \tag{5}$$

$$(1+\nu)\nabla^2\sigma_z + \frac{\partial^2\Theta}{\partial z^2} = -\frac{(\alpha_x + \alpha_y)E}{(1-\nu)}\frac{\partial^2 c}{\partial z^2}, \tag{6}$$

$$(1+\nu)\nabla^2\tau_{yz} + \frac{\partial^2\Theta}{\partial y \partial z} = 0, \tag{7}$$

$$(1+\nu)\nabla^2\tau_{xz} + \frac{\partial^2\Theta}{\partial x \partial z} = 0, \tag{8}$$

$$(1+\nu)\nabla^2\tau_{xy} + \frac{\partial^2\Theta}{\partial x \partial y} = 0, \tag{9}$$

where $\nabla^2 = \partial^2/\partial x^2 + \partial^2/\partial y^2 + \partial^2/\partial z^2$. The right-hand sides of Equations (4)–(6) are the non-standard terms in the compatibility conditions. The boundary conditions are

$$u = \frac{\partial v}{\partial x} = \frac{\partial w}{\partial x} = 0 \qquad \text{on } x = 0, \tag{10}$$

$$\sigma_x = \tau_{xy} = \tau_{xz} = 0 \qquad \text{on } x = L, \tag{11}$$

$$v = \frac{\partial u}{\partial y} = \frac{\partial w}{\partial y} = 0 \qquad \text{on } y = 0, \tag{12}$$

$$\tau_{xy} = \sigma_y = \tau_{yz} = 0 \qquad \text{on } y = W, \tag{13}$$

$$\tau_{xz} = \tau_{yz} = \sigma_z = 0 \qquad \text{on } z = \pm h. \tag{14}$$

If the concentration is linear $c(z,t) = C_1 + C_2 z$, we obtain an exact (stress-free) solution, namely $u = \alpha_x x(C_1 + C_2 z)$, $v = \alpha_y y(C_1 + C_2 z)$ and $w = \alpha_z(C_1 z + C_2 z^2/2) - C_2(\alpha_x x^2 + \alpha_y y^2)/2$ (*cf.* [6]).

3. Asymptotic analysis

3.1. INTRODUCTION

A schematic representation of the four asymptotic regions to be described in this section is shown in Figure 2. A quarter of the panel to be studied is shown; $\hat{x} = 0$ and $\hat{y} = 0$ are planes of symmetry. Region I occupies the majority of the panel. There are two thin boundary-layer regions II and III which run along $x = L$ and $y = W$, respectively. A very small corner region in the neighbourhood of the point $x = L$, $y = W$ is denoted by region IV. The analysis in Subsections 3.2 to 3.5 predict the form of the stress tensor in regions I, II and III. Moreover, we shall show that the solution in these regions is unique. In Subsection 3.6, the displacements are deduced from the stresses.

3.2. OUTER EXPANSION: REGION I

We seek the outer expansion which is a solution of the overdetermined system (3)–(9). We transform to dimensionless variables via $x = L\hat{x}$, $y = L\hat{y}$, $z = h\hat{z}$, $t = \tau\hat{t}$, $u = \delta h\hat{u}$, $v = \delta h\hat{v}$, $w = h\hat{w}$, $\sigma_x = \delta^2 E\hat{\sigma}_x$, $\sigma_y = \delta^2 E\hat{\sigma}_y$, $\sigma_z = \delta^4 E\hat{\sigma}_z$, $\tau_{xy} = \delta^2 E\hat{\tau}_{xy}$, $\tau_{xz} = \delta^3 E\hat{\tau}_{xz}$, $\tau_{yz} = \delta^3 E\hat{\tau}_{yz}$ and $c = \delta^2\hat{c}/\alpha_z$, where $\delta = h/L$ and τ is the time-scale of a few days. The equations for conservation of momentum become

$$\frac{\partial\hat{\sigma}_x}{\partial\hat{x}} + \frac{\partial\hat{\tau}_{xy}}{\partial\hat{y}} + \frac{\partial\hat{\tau}_{xz}}{\partial\hat{z}} = 0, \qquad \frac{\partial\hat{\tau}_{xy}}{\partial\hat{x}} + \frac{\partial\hat{\sigma}_y}{\partial\hat{y}} + \frac{\partial\hat{\tau}_{yz}}{\partial\hat{z}} = 0, \qquad \frac{\partial\hat{\tau}_{xz}}{\partial\hat{x}} + \frac{\partial\hat{\tau}_{yz}}{\partial\hat{y}} + \frac{\partial\hat{\sigma}_z}{\partial\hat{z}} = 0,$$

and the compatibility conditions transform to

$$(1+\nu)\left(\delta^2\left(\frac{\partial^2}{\partial\hat{x}^2} + \frac{\partial^2}{\partial\hat{y}^2}\right) + \frac{\partial^2}{\partial\hat{z}^2}\right)\hat{\sigma}_x + \delta^2\frac{\partial^2}{\partial\hat{x}^2}(\hat{\sigma}_x + \hat{\sigma}_y + \delta^2\hat{\sigma}_z) = -\frac{(\alpha_x + \nu\alpha_y)}{\alpha_z(1-\nu)}\frac{\partial^2\hat{c}}{\partial\hat{z}^2},$$

$$(1+\nu)\left(\delta^2\left(\frac{\partial^2}{\partial\hat{x}^2} + \frac{\partial^2}{\partial\hat{y}^2}\right) + \frac{\partial^2}{\partial\hat{z}^2}\right)\hat{\sigma}_y + \delta^2\frac{\partial^2}{\partial\hat{y}^2}(\hat{\sigma}_x + \hat{\sigma}_y + \delta^2\hat{\sigma}_z) = -\frac{(\alpha_y + \nu\alpha_x)}{\alpha_z(1-\nu)}\frac{\partial^2\hat{c}}{\partial\hat{z}^2},$$

$$(1+\nu)\left(\delta^2\left(\frac{\partial^2}{\partial\hat{x}^2} + \frac{\partial^2}{\partial\hat{y}^2}\right) + \frac{\partial^2}{\partial\hat{z}^2}\right)\delta^2\hat{\sigma}_z + \frac{\partial^2}{\partial\hat{z}^2}(\hat{\sigma}_x + \hat{\sigma}_y + \delta^2\hat{\sigma}_z) = -\frac{(\alpha_x + \alpha_y)}{\alpha_z(1-\nu)}\frac{\partial^2\hat{c}}{\partial\hat{z}^2},$$

$$(1+\nu)\left(\delta^2\left(\frac{\partial^2}{\partial\hat{x}^2} + \frac{\partial^2}{\partial\hat{y}^2}\right) + \frac{\partial^2}{\partial\hat{z}^2}\right)\hat{\tau}_{yz} + \frac{\partial^2}{\partial\hat{y}\partial\hat{z}}(\hat{\sigma}_x + \hat{\sigma}_y + \delta^2\hat{\sigma}_z) = 0,$$

$$(1+\nu)\left(\delta^2\left(\frac{\partial^2}{\partial\hat{x}^2} + \frac{\partial^2}{\partial\hat{y}^2}\right) + \frac{\partial^2}{\partial\hat{z}^2}\right)\hat{\tau}_{xz} + \frac{\partial^2}{\partial\hat{x}\partial\hat{z}}(\hat{\sigma}_x + \hat{\sigma}_y + \delta^2\hat{\sigma}_z) = 0,$$

$$(1+\nu)\left(\delta^2\left(\frac{\partial^2}{\partial\hat{x}^2} + \frac{\partial^2}{\partial\hat{y}^2}\right) + \frac{\partial^2}{\partial\hat{z}^2}\right)\hat{\tau}_{xy} + \delta^2\frac{\partial^2}{\partial\hat{y}\partial\hat{z}}(\hat{\sigma}_x + \hat{\sigma}_y + \delta^2\hat{\sigma}_z) = 0,$$

The displacements are determined from the non-dimensional equations

$$\frac{\partial\hat{u}}{\partial\hat{x}} = \hat{\sigma}_x - \nu(\hat{\sigma}_y + \delta^2\hat{\sigma}_z) + \frac{\alpha_x}{\alpha_z}\hat{c}(\hat{z},\hat{t}), \frac{\partial\hat{v}}{\partial\hat{y}} = \hat{\sigma}_y - \nu(\hat{\sigma}_x + \delta^2\hat{\sigma}_z) + \frac{\alpha_y}{\alpha_z}\hat{c}(\hat{z},\hat{t}),$$

$$\frac{\partial\hat{w}}{\partial\hat{z}} = \delta^4\hat{\sigma}_z - \nu\delta^2(\hat{\sigma}_x + \hat{\sigma}_y) + \delta^2\hat{c}(\hat{z},\hat{t}),$$

$$\hat{\tau}_{xy} = \frac{1}{2(1+\nu)}\left(\frac{\partial \hat{u}}{\partial \hat{y}} + \frac{\partial \hat{v}}{\partial \hat{x}}\right), \quad \delta^2\hat{\tau}_{xz} = \frac{1}{2(1+\nu)}\left(\frac{\partial \hat{u}}{\partial \hat{z}} + \frac{\partial \hat{w}}{\partial \hat{x}}\right),$$

$$\delta^2\hat{\tau}_{yz} = \frac{1}{2(1+\nu)}\left(\frac{\partial \hat{v}}{\partial \hat{z}} + \frac{\partial \hat{w}}{\partial \hat{y}}\right).$$

We obtain the leading-order solution for stresses

$$\hat{\sigma}_x \sim -\frac{(\alpha_x + \nu\alpha_y)}{\alpha_z(1-\nu^2)}\hat{c}(\hat{z},\hat{t}) + \mathcal{A}\hat{z} + \mathcal{B}, \qquad \hat{\sigma}_y \sim -\frac{(\alpha_y + \nu\alpha_x)}{\alpha_z(1-\nu^2)}\hat{c}(\hat{z},\hat{t}) + \mathcal{D}\hat{z} + \mathcal{E}, \tag{15}$$

$\hat{\tau}_{xy} = O(\delta^2)$, $\hat{\tau}_{xz} = O(\delta^2)$, $\hat{\tau}_{yz} = O(\delta^2)$ and $\hat{\sigma}_z = O(\delta^2)$ as $\delta^2 \to 0$ where $\mathcal{A}$, $\mathcal{B}$, $\mathcal{D}$ and $\mathcal{E}$ are unknown constants. The corresponding leading-order displacements are given by

$$\begin{aligned} &\hat{u} \sim (\mathcal{A} - \nu\mathcal{D})\hat{x}\hat{z} + (\mathcal{B} - \nu\mathcal{E})\hat{x}, \quad \hat{v} \sim (\mathcal{D} - \nu\mathcal{A})\hat{y}\hat{z} + (\mathcal{E} - \nu\mathcal{B})\hat{y}, \\ &\hat{w} \sim -\frac{\hat{x}^2}{2}(\mathcal{A} - \nu\mathcal{D}) - \frac{\hat{y}^2}{2}(\mathcal{D} - \nu\mathcal{A}), \end{aligned} \tag{16}$$

where $\mathcal{A}$, $\mathcal{B}$, $\mathcal{D}$ and $\mathcal{E}$ depend on the moisture concentration.

3.3. Boundary-layer expansion at $x = L$: Region II

We now transform to dimensionless variables via $x = L - h\bar{x}$, $\sigma_x = \delta^2 E\bar{\sigma}_x$, $\sigma_y = \delta^2 E\bar{\sigma}_y$, $\sigma_z = \delta^2 E\bar{\sigma}_z$, $\tau_{xy} = \delta E\bar{\tau}_{xy}$, $\tau_{xz} = \delta^2 E\bar{\tau}_{xz}$ and $\tau_{yz} = \delta E\bar{\tau}_{yz}$. The equations for conservation of momentum become

$$-\frac{\partial \bar{\sigma}_x}{\partial \bar{x}} + \frac{\partial \bar{\tau}_{xy}}{\partial \hat{y}} + \frac{\partial \bar{\tau}_{xz}}{\partial \hat{z}} = 0, \quad -\frac{\partial \bar{\tau}_{xy}}{\partial \bar{x}} + \delta^2\frac{\partial \bar{\sigma}_y}{\partial \hat{y}} + \frac{\partial \bar{\tau}_{yz}}{\partial \hat{z}} = 0, \quad -\frac{\partial \bar{\tau}_{xz}}{\partial \bar{x}} + \frac{\partial \bar{\tau}_{yz}}{\partial \hat{y}} + \frac{\partial \bar{\sigma}_z}{\partial \hat{z}} = 0,$$

and the compatibility conditions transform to

$$(1+\nu)\left(\frac{\partial^2}{\partial \bar{x}^2} + \delta^2\frac{\partial^2}{\partial \hat{y}^2} + \frac{\partial^2}{\partial \hat{z}^2}\right)\bar{\sigma}_x + \frac{\partial^2}{\partial \bar{x}^2}(\bar{\sigma}_x + \bar{\sigma}_y + \bar{\sigma}_z) = -\frac{(\alpha_x + \nu\alpha_y)}{\alpha_z(1-\nu)}\frac{\partial^2 \hat{c}}{\partial \hat{z}^2},$$

$$(1+\nu)\left(\frac{\partial^2}{\partial \bar{x}^2} + \delta^2\frac{\partial^2}{\partial \hat{y}^2} + \frac{\partial^2}{\partial \hat{z}^2}\right)\bar{\sigma}_y + \delta^2\frac{\partial^2}{\partial \hat{y}^2}(\bar{\sigma}_x + \bar{\sigma}_y + \bar{\sigma}_z) = -\frac{(\alpha_y + \nu\alpha_x)}{\alpha_z(1-\nu)}\frac{\partial^2 \hat{c}}{\partial \hat{z}^2},$$

$$(1+\nu)\left(\frac{\partial^2}{\partial \bar{x}^2} + \delta^2\frac{\partial^2}{\partial \hat{y}^2} + \frac{\partial^2}{\partial \hat{z}^2}\right)\bar{\sigma}_z + \frac{\partial^2}{\partial \hat{z}^2}(\bar{\sigma}_x + \bar{\sigma}_y + \bar{\sigma}_z) = -\frac{(\alpha_x + \alpha_y)}{\alpha_z(1-\nu)}\frac{\partial^2 \hat{c}}{\partial \hat{z}^2},$$

$$(1+\nu)\left(\frac{\partial^2}{\partial \bar{x}^2} + \delta^2\frac{\partial^2}{\partial \hat{y}^2} + \frac{\partial^2}{\partial \hat{z}^2}\right)\bar{\tau}_{yz} + \delta^2\frac{\partial^2}{\partial \hat{y}\partial \hat{z}}(\bar{\sigma}_x + \bar{\sigma}_y + \bar{\sigma}_z) = 0,$$

$$(1+\nu)\left(\frac{\partial^2}{\partial \bar{x}^2} + \delta^2\frac{\partial^2}{\partial \hat{y}^2} + \frac{\partial^2}{\partial \hat{z}^2}\right)\bar{\tau}_{xz} - \frac{\partial^2}{\partial \bar{x}\partial \hat{z}}(\bar{\sigma}_x + \bar{\sigma}_y + \bar{\sigma}_z) = 0,$$

$$(1+\nu)\left(\frac{\partial^2}{\partial \bar{x}^2} + \delta^2\frac{\partial^2}{\partial \hat{y}^2} + \frac{\partial^2}{\partial \hat{z}^2}\right)\bar{\tau}_{xy} - \delta^2\frac{\partial^2}{\partial \bar{x}\partial \hat{y}}(\bar{\sigma}_x + \bar{\sigma}_y + \bar{\sigma}_z) = 0.$$

The distinguished limit in this boundary layer includes all the terms that balance at leading order in region I. Therefore, the solution in region II is uniformly valid across regions I and II. We have the leading-order solution

$$\bar{\sigma}_x \sim \frac{\partial^2\phi}{\partial\hat{z}^2}, \quad \bar{\sigma}_y \sim \nu\left(\frac{\partial^2}{\partial\bar{x}^2}+\frac{\partial^2}{\partial\hat{z}^2}\right)\phi - \frac{\alpha_y\hat{c}(\hat{z},\hat{t})}{\alpha_z} + (\mathcal{D}-\nu\mathcal{A})\hat{z} + (\mathcal{E}-\nu\mathcal{B}),$$
$$\bar{\sigma}_z \sim \frac{\partial^2\phi}{\partial\bar{x}^2}, \quad \bar{\tau}_{xz} \sim \frac{\partial^2\phi}{\partial\bar{x}\partial\hat{z}}, \tag{17}$$

$\bar{\tau}_{xy} = O(\delta^2)$ and $\bar{\tau}_{yz} = O(\delta^2)$ where the stress function $\phi(\bar{x},\hat{z})$ (cf. the stress function in the homogeneous problem 1A of [5] is given by

$$\left(\frac{\partial^2}{\partial\bar{x}^2}+\frac{\partial^2}{\partial\hat{z}^2}\right)^2\phi = -\frac{(\alpha_x+\nu\alpha_y)}{\alpha_z(1-\nu^2)}\frac{\partial^2\hat{c}}{\partial\hat{z}^2}, \tag{18}$$

with the boundary conditions

$$\text{on } \hat{z}=-1,1: \frac{\partial^2\phi}{\partial\bar{x}\partial\hat{z}} = \frac{\partial^2\phi}{\partial\bar{x}^2} = 0 \text{ for } 0<\bar{x}, \tag{19}$$

$$\text{on } \bar{x}=0: \frac{\partial^2\phi}{\partial\bar{x}\partial\hat{z}} = \frac{\partial^2\phi}{\partial\hat{z}^2} = 0 \text{ for } -1<\hat{z}<1, \tag{20}$$

$$\text{as } \bar{x}\to\infty: \frac{\partial^2\phi}{\partial\bar{x}\partial\hat{z}}\to 0, \quad \frac{\partial^2\phi}{\partial\hat{z}^2}\to -\frac{(\alpha_x+\nu\alpha_y)}{\alpha_z(1-\nu^2)}\hat{c}(\hat{z},\hat{t}) + \mathcal{A}\hat{z} + \mathcal{B} \text{ for } -1<\hat{z}<1. \tag{21}$$

Conditions (21) were obtained by matching with region I. The displacements are determined from the non-dimensional equations

$$-\frac{\partial\hat{u}}{\partial\bar{x}} = \delta\left(\bar{\sigma}_x - \nu(\bar{\sigma}_y+\bar{\sigma}_z) + \frac{\alpha_x}{\alpha_z}\hat{c}\right), \frac{\partial\hat{v}}{\partial\hat{y}} = \bar{\sigma}_y - \nu(\bar{\sigma}_x+\bar{\sigma}_z) + \frac{\alpha_y}{\alpha_z}\hat{c},$$
$$\frac{\partial\hat{w}}{\partial\hat{z}} = \delta^2\left(\bar{\sigma}_z - \nu(\bar{\sigma}_x+\bar{\sigma}_y) + \hat{c}\right),$$
$$\bar{\tau}_{xy} = \frac{1}{2(1+\nu)}\left(\delta\frac{\partial\hat{u}}{\partial\hat{y}} - \frac{\partial\hat{v}}{\partial\bar{x}}\right), \quad \delta^2\bar{\tau}_{xz} = \frac{1}{2(1+\nu)}\left(\delta\frac{\partial\hat{u}}{\partial\hat{z}} - \frac{\partial\hat{w}}{\partial\bar{x}}\right),$$
$$\bar{\tau}_{yz} = \frac{1}{2(1+\nu)}\left(\frac{\partial\hat{v}}{\partial\hat{z}} + \frac{\partial\hat{w}}{\partial\hat{y}}\right).$$

We note that there are no rapid changes in the displacements across this boundary layer. The detailed structure of the stresses in the boundary layer will only be relevant in determining the matching constants.

3.4. Other boundary-layer expansions: Regions III and IV

The boundary layer at $y = W$ is similar to the layer at $x = L$. We transform to dimensionless variables via $y = W-h\bar{y}$, $\sigma_x = \delta^2 E\sigma_x^*$, $\sigma_y = \delta^2 E\sigma_y^*$, $\sigma_z = \delta^2 E\sigma_z^*$, $\tau_{xy} = \delta E\tau_{xy}^*$, $\tau_{xz} = \delta E\tau_{xz}^*$ and $\tau_{yz} = \delta^2 E\tau_{yz}^*$. By symmetry the solutions may be derived from (17) by replacing x, y, $\mathcal{A}$, $\mathcal{B}$, $\mathcal{D}$ and $\mathcal{E}$ by y, x, $\mathcal{D}$, $\mathcal{E}$, $\mathcal{A}$ and $\mathcal{B}$, respectively. The composite expansion across regions I, II and III may be obtained by adding the leading-order solutions in regions II and III, then subtracting the leading-order solution in region I.

There is also a boundary layer at $x = L$ and $y = W$ ($\bar{x} > 0$ and $\bar{y} > 0$). We now transform to dimensionless dependent variables via $\sigma_x = \delta^2 E\sigma_x'$, $\sigma_y = \delta^2 E\sigma_y'$, $\sigma_z = \delta^2 E\sigma_z'$,

$\tau_{xy} = \delta^2 E\tau'_{xy}$, $\tau_{xz} = \delta^2 E\tau'_{xz}$ and $\tau_{yz} = \delta^2 E\tau'_{yz}$. In this region a full balance is obtained in (3)–(9). The corner region does not possess an appropriate stress function and the mathematical theory is less elegant than in regions II and III. Matching the expansion in this region will not be necessary to determine the unknown constants $\mathcal{A}$, $\mathcal{B}$, $\mathcal{D}$ and $\mathcal{E}$ or the form of the stresses in regions II and III.

3.5. MATCHING CONSTANTS

The solution of the boundary-value problem (18)–(21) would determine the matching constants $\mathcal{A}$ and $\mathcal{B}$. We derive conditions under which a unique solution exists. The transformation

$$\psi = \phi - \int_{z'=-1}^{\hat{z}} \int_{z''=-1}^{z'} \left(-\frac{(\alpha_x + \nu\alpha_y)}{\alpha_z(1-\nu^2)} \hat{c}(z'', \hat{t}) + \mathcal{A}z'' + \mathcal{B} \right) \mathrm{d}z''\mathrm{d}z' - \frac{\partial\phi}{\partial\bar{x}}(0,-1)\bar{x} - \frac{\partial\phi}{\partial\hat{z}}(0,-1)(\hat{z}+1) - \phi(0,-1)$$

leads to the problem

$$\left(\frac{\partial^2}{\partial\bar{x}^2} + \frac{\partial^2}{\partial\hat{z}^2} \right)^2 \psi = 0, \tag{22}$$

with the boundary conditions

$$\text{on} \quad \hat{z} = -1, 1 : \psi = \frac{\partial\psi}{\partial\hat{z}} = 0 \qquad \text{for } \bar{x} > 0, \tag{23}$$

$$\text{on} \quad \bar{x} = 0 : \frac{\partial\psi}{\partial\bar{x}} = 0,$$

$$\psi = \frac{(\alpha_x + \nu\alpha_y)}{\alpha_z(1-\nu^2)} \int_{z'=-1}^{\hat{z}} \int_{z''=-1}^{z'} \hat{c}(z'', \hat{t})\mathrm{d}z''\mathrm{d}z' - \frac{(\hat{z}+1)^2}{6} \left(\mathcal{A}(\hat{z}-2) + 3\mathcal{B} \right) \tag{24}$$

$$\text{for} \quad -1 < \hat{z} < 1,$$

$$\text{as} \quad \bar{x} \to \infty : \psi \to 0, \qquad \frac{\partial\psi}{\partial\bar{x}} \to 0 \ \text{ for } \ -1 < \hat{z} < 1, \tag{25}$$

provided the matching constants $\mathcal{A}$ and $\mathcal{B}$ are given by

$$\mathcal{A} = \frac{3(\alpha_x + \nu\alpha_y)}{2\alpha_z(1-\nu^2)} \int_{\hat{z}=-1}^{1} \hat{z}\hat{c}(\hat{z}, \hat{t})\mathrm{d}\hat{z}, \qquad \mathcal{B} = \frac{(\alpha_x + \nu\alpha_y)}{2\alpha_z(1-\nu^2)} \int_{\hat{z}=-1}^{1} \hat{c}(\hat{z}, \hat{t})\mathrm{d}\hat{z}. \tag{26}$$

The Fredholm alternative guarantees that (22)–(25) has a unique solution. By symmetry, $\mathcal{D}$ and $\mathcal{E}$ are given by

$$\mathcal{D} = \frac{3(\alpha_y + \nu\alpha_x)}{2\alpha_z(1-\nu^2)} \int_{\hat{z}=-1}^{1} \hat{z}\hat{c}(\hat{z}, \hat{t})\mathrm{d}\hat{z}, \qquad \mathcal{E} = \frac{(\alpha_y + \nu\alpha_x)}{2\alpha_z(1-\nu^2)} \int_{\hat{z}=-1}^{1} \hat{c}(\hat{z}, \hat{t})\mathrm{d}\hat{z}. \tag{27}$$

A physical approach to determining the matching constants is to apply the divergence theorem to the first equation in (3) and

$$\frac{\partial}{\partial x}(z\sigma_x) + \frac{\partial}{\partial y}(z\tau_{xy}) + \frac{\partial}{\partial z}(z\tau_{xz}) = \tau_{xz},$$

and then non-dimensionalising, to obtain

$$\int_{\hat{z}=-1}^{1} \hat{\sigma}_x \mathrm{d}\hat{z} = O(\delta^2), \qquad \int_{\hat{z}=-1}^{1} \hat{z}\hat{\sigma}_x \mathrm{d}\hat{z} = \int_{\bar{x}=0}^{\infty} \int_{\hat{z}=-1}^{1} \bar{\tau}_{xz} \mathrm{d}\hat{z}\mathrm{d}\bar{x} + O(\delta^2), \tag{28}$$

respectively. We note that substituting the solution (17) for $\bar{\tau}_{xz}$ will set the first integral on the right-hand side of the second equation in (28) equal to zero, that is the stress resultant and bending moment are negligible at leading order.

3.6. DISPLACEMENTS

The displacements may now be deduced by substituting (26)–(27) in (16). In dimensional form the displacements become

$$u \sim \frac{3\alpha_x xz}{2h^3} \int_{z=-h}^{h} zc(z,t)\mathrm{d}z + \frac{\alpha_x x}{2h} \int_{z=-h}^{h} c(z,t)\mathrm{d}z, \tag{29}$$

$$v \sim \frac{3\alpha_y yz}{2h^3} \int_{z=-h}^{h} zc(z,t)\mathrm{d}z + \frac{\alpha_y y}{2h} \int_{z=-h}^{h} c(z,t)\mathrm{d}z, \tag{30}$$

$$w \sim -\frac{3(\alpha_x x^2 + \alpha_y y^2)}{4h^3} \int_{z=-h}^{h} zc(z,t)\mathrm{d}z. \tag{31}$$

The panel approximately warps into a circular arc along the x-axis and the y-axis with radius

$$\frac{2h^3}{3\alpha_x \int_{z=-h}^{h} zc(z,t)\mathrm{d}z}, \qquad \frac{2h^3}{3\alpha_y \int_{z=-h}^{h} zc(z,t)\mathrm{d}z},$$

respectively. Experimental observations indicate that panels warp in this manner (see Subsection 5.1.1). For the special case where concentration is linear, (29)–(31) reduces to the exact (stress-free) solution (see Section 2).

The presence of the moment of moisture concentration in the expression for warp indicates the significance of surface effects which take place over a relatively short time-scale (in comparison to the time-scale for the diffusion of moisture). We note that the panel warp may be reduced by decreasing the moment of the moisture concentration or by increasing the panel thickness.

The parameters α_x and α_y may be determined from the steady-state extension (or contraction) in the length and width in response to a constant increase (or decrease) in relative humidity across the panel thickness (see Subsection 5.1.1).

It remains to model the moisture concentration in interior and exterior applications. Once the moisture concentration has been predicted, deformation may be easily calculated using (29)–(31).

4. Moisture transport in exterior applications

4.1. PROBLEM FORMULATION

We adopt the following assumptions: (i) swelling or shrinkage in the transverse direction is negligible (w is independent of z at leading order in (31)) and (ii) the material is homogeneous.

Temperature variations now play an important rôle and must be included. The moisture-transport model can be described by two dependent variables: the moisture concentration $c(z,t)$ and the temperature $T(z,t)$. These satisfy the following equations together with the appropriate constitutive assumption for the moisture diffusion coefficient $D(T)$

$$\frac{\partial c}{\partial t} = \frac{\partial}{\partial z}\left(D\frac{\partial c}{\partial z}\right) \quad \text{with} \quad D = D_0 \exp\left(-\frac{T_r}{T}\right),$$

$$\rho c_p \frac{\partial T}{\partial t} = \frac{\partial}{\partial z}\left(k\frac{\partial T}{\partial z}\right),$$

where c_p is the specific heat capacity, k is the thermal conductivity, D_0 is the diffusion coefficient at temperatures much larger than the reference temperature T_r. These equations require boundary conditions at $z = \pm h$. A décor layer is usually present on the surface of a panel. These layers are typically very thin and play no rôle in the deformation of the panel. However, the décor material is also chosen to reduce the diffusion of moisture into the panel, so Robin conditions are necessary. The sides of the panel may or may not be well ventilated, so the ambient moisture concentration and temperature are not identical on $z = \pm h$. Another asymmetry arises from absorbed solar radiation on one side of the panel. We assume a balance of moisture and thermal flux at the décor boundaries, so that

$$\text{on } z = h : D\frac{\partial c}{\partial z} = H(c_R(t) - c), \qquad -k\frac{\partial T}{\partial z} = \gamma(T - T_R(t)) - S(t),$$

$$\text{on } z = -h : D\frac{\partial c}{\partial z} = H(c - c_L(t)), \qquad -k\frac{\partial T}{\partial z} = \gamma(T_L(t) - T),$$

with

$$H = H_0 \exp\left(-\frac{T_H}{T}\right),$$

where H_0 is the mass-transfer coefficient at temperatures much larger than the reference temperature T_H, γ is the heat-transfer coefficient, $c_L(t)$ ($c_R(t)$) is the ambient moisture concentration on the left-hand (right-hand) side, $T_L(t)$ ($T_R(t)$) is the ambient temperature on the left-hand (right-hand) side and $S(t)$ is the thermal flux resulting from absorbed radiation at the décor surface. The initial conditions are taken to be

$$c(z,0) = c_R(0), \qquad T(z,0) = T_R(0).$$

4.2. NON-DIMENSIONALISATION

We now non-dimensionalise these equations enabling the dominant balances to be identified. The maximum value of the moisture uptake is denoted by $c_{\max}$, a representative temperature rise by ΔT and the maximum value of the thermal flux from radiation by $S_{\max}$. We introduce a time-scale $\tau^* = 1\ \text{day}/2\pi$. We transform to dimensionless variables via $z = h\hat{z}$, $t = \tau^* t^*$, $c = c_R(0) + (c_{\max} - c_R(0))c^*$, $T = T_R(0) + \Delta T T^*$, $c_L(t) = c_R(0) + (c_{\max} - c_R(0))c_L^*$, $c_R(t) = c_R(0) + (c_{\max} - c_R(0))c_R^*$, $T_L(t) = T_R(0) + \Delta T T_L^*$, $T_R(t) = T_R(0) + \Delta T T_R^*$ and $S = S_{\max} S^*$. The problem becomes

Table 2. Dimensionless parameters for moisture transport in exterior applications (where some values are reliable and some best estimates)

Symbol	Definition	Typical Value
ν	$\Delta T/T_R(0)$	7×10^{-2}
β	$T_r\Delta T/T_R(0)^2$	1
β_H	$T_H\Delta T/T_R(0)^2$	1
$\bar{D}$	$D_0\tau^*\exp(-T_r/T_R(0))/h^2$	10^{-4}
F	$k\tau^*/\rho c_p h^2$	50
$\bar{D}^{1/2}\bar{K}$	$D_0\exp\left((T_H-T_r)/T_R(0)\right)/hH_0$	7×10^{-2}
$\bar{B}/F$	$\gamma h/k$	2×10^{-2}
$\bar{Q}/F$	$hS_{\max}/k\Delta T$	2×10^{-2}
r	$2\pi\tau^*/\bar{D}$(1 year)	20

$$\frac{\partial c^*}{\partial t^*}=\bar{D}\frac{\partial}{\partial\hat{z}}\left(\exp\left(\frac{\beta T^*}{1+\nu T^*}\right)\frac{\partial c^*}{\partial\hat{z}}\right), \tag{32}$$

$$\frac{\partial T^*}{\partial t^*}=F\frac{\partial^2 T^*}{\partial\hat{z}^2}, \tag{33}$$

with boundary conditions

$$\text{on } \hat{z}=1:\ \bar{D}^{1/2}\bar{K}\exp\left(\frac{\beta T^*}{1+\nu T^*}\right)\frac{\partial c^*}{\partial\hat{z}}=\exp\left(\frac{\beta_H T^*}{1+\nu T^*}\right)\left(c_R^*(t^*,\tilde{t})-c^*\right), \tag{34}$$

$$\text{on } \hat{z}=1:\ -\frac{\partial T^*}{\partial\hat{z}}=\frac{\bar{B}}{F}(T^*-T_R^*(t^*,\tilde{t}))-\frac{\bar{Q}}{F}S^*(t^*,\tilde{t}), \tag{35}$$

$$\text{on } \hat{z}=-1:\ \bar{D}^{1/2}\bar{K}\exp\left(\frac{\beta T^*}{1+\nu T^*}\right)\frac{\partial c^*}{\partial\hat{z}}=\exp\left(\frac{\beta_H T^*}{1+\nu T^*}\right)\left(c^*-c_L^*(t^*,\tilde{t})\right), \tag{36}$$

$$\text{on } \hat{z}=-1:\ -\frac{\partial T^*}{\partial\hat{z}}=\frac{\bar{B}}{F}(T_L^*(t^*,\tilde{t})-T^*), \tag{37}$$

and initial conditions

$$c^*(\hat{z},0,0)=0,\qquad T^*(\hat{z},0,0)=0. \tag{38}$$

The dimensionless constants ν, β, β_H, $\bar{D}$, F, $\bar{K}$, $\bar{B}$ and $\bar{Q}$ are defined, and typical values given, in Table 2; the constraint $\bar{D}\ll 1/F\ll 1$ typically holds in practice. The thermal conduction time-scale ($\rho c_p h^2/k\sim 300$s), the time-scale of one day and the diffusion time-scale ($h^2\exp(T_r/T_R(0))/D_0\sim 4$ years) are the three relevant time-scales in exterior applications. Time is described by two variables: the intermediate time-scale t^* which corresponds to the daily periodic variation and the longest time-scale $\tilde{t}$ ($\tilde{t}=\bar{D}t^*$) which corresponds to diffusion. The solution is periodic in t^*, with period 2π, at leading order.

4.3. ASYMPTOTIC ANALYSIS

4.3.1. *Temperature*

We introduce an expansion for temperature of the form $T^* \sim T_0(t^*, \tilde{t}) + T_1/F$. Equation (33) implies

$$\frac{\partial T_1}{\partial \hat{z}} = \frac{\partial T_0}{\partial t^*}\hat{z} + A_1(t^*, \tilde{t}),$$

which may be substituted in (35) and (37) to give

$$\frac{\partial T_0}{\partial t^*} + \bar{B}T_0 = \frac{\bar{B}}{2}(T_L^*(t^*, \tilde{t}) + T_R^*(t^*, \tilde{t})) + \frac{\bar{Q}}{2}S^*(t^*, \tilde{t}),$$

with solution

$$T_0 = \exp(-\bar{B}t^*)\int_{s=0}^{t^*} \exp(\bar{B}s)\left[\frac{\bar{B}}{2}(T_L^*(s, \tilde{t}) + T_R^*(s, \tilde{t})) + \frac{\bar{Q}}{2}S^*(s, \tilde{t})\right]\mathrm{d}s.$$

It remains to obtain the moisture concentration which depends on the value of $\beta_H - \beta$.

4.3.2. *Moisture concentration: $\beta_H - \beta = O(1)$*

In this parameter régime the leading-order term for temperature must be used in combination with a numerical solution of (32), (34), (36) and $(38)_1$. The numerical solution has to take into account the short time-scale of a day (in boundary layers adjacent to the décor layer with length $O(\bar{D}^{1/2})$) and the long time-scale of 4 years (throughout the panel).

4.3.3. *Moisture concentration: $\beta_H - \beta = o(1)$*

Inner expansion

A multiple-scale expansion in time and boundary-layer expansion in space is possible in this parameter régime. Firstly, we consider the boundary layers. The inner expansions at the two boundaries $\hat{z} = \pm 1$ are similar, therefore we will only describe the problem in the neighbourhood of $\hat{z} = -1$. We perform the stretching transformation $\hat{z} = -1 + \bar{D}^{1/2}Z$ and introduce the expansion $c^* \sim C_0(Z, t^*, \tilde{t})$, to obtain the leading-order problem

$$\frac{\partial C_0}{\partial t^*} = \exp\left(\frac{\beta T_0}{1 + \nu T_0}\right)\frac{\partial^2 C_0}{\partial Z^2}, \tag{39}$$

with boundary conditions

$$\bar{K}\frac{\partial C_0}{\partial Z} = C_0(0, t^*, \tilde{t}) - c_L^*(t^*, \tilde{t}), \qquad C_0 \to c_{BL}(\tilde{t}) \text{ as } Z \to \infty, \tag{40}$$

where $c_{BL}(\tilde{t})$ is to be determined. The initial condition is $C_0(Z, 0, 0) = 0$. Periodicity in t^* demands that

$$\int_0^{2\pi} \frac{\partial C_0}{\partial t^*}\mathrm{d}t^* = 0,$$

so (39) and $(40)_2$ implies

$$\int_0^{2\pi} \exp\left(\frac{\beta T_0}{1 + \nu T_0}\right) C_0 \mathrm{d}t^* = A_0(\tilde{t}).$$

Integrating the boundary conditions (40), we obtain the result

$$c_{BL}(\tilde{t}) =< c_L^*(t^*, \tilde{t}) > / < 1 >,$$

and similarly

$$c_{BR}(\tilde{t}) =< c_R^*(t^*, \tilde{t}) > / < 1 >,$$

where we define the average

$$< \cdot >= \frac{1}{2\pi} \int_0^{2\pi} \cdot \exp\left(\frac{\beta T_0}{1 + \nu T_0}\right) \mathrm{d}t^*.$$

We note that the expressions derived for $c_{BL}(\tilde{t})$ and $c_{BR}(\tilde{t})$ are also valid in the limit $\bar{K} \ll 1$ irrespective of the value of $\beta_H - \beta$.

Outer expansion

We now consider the outer region and introduce the expansion $c^* \sim c_0(\hat{z}, \tilde{t})$. Elimination of the secular terms in (32) leads to the equation for the leading-order term for moisture concentration

$$\frac{\partial c_0}{\partial \tilde{t}} =< 1 > \frac{\partial^2 c_0}{\partial \hat{z}^2},$$

with the boundary conditions $c_0(-1, \tilde{t}) = c_{BL}(\tilde{t})$ and $c_0(1, \tilde{t}) = c_{BR}(\tilde{t})$. The averaged term $< 1 >$ is the effective moisture diffusion coefficient. The change of variable defined by

$$t_1 = \int_0^{\tilde{t}} < 1 > \mathrm{d}\tilde{t}', \tag{41}$$

results in a problem with constant diffusion coefficient for the moisture concentration at leading order, namely

$$\frac{\partial c_0}{\partial t_1} = \frac{\partial^2 c_0}{\partial \hat{z}^2}, \quad c_0(-1, t_1) = c_{TL}(t_1), \quad c_0(1, t_1) = c_{TR}(t_1), \quad c_0(\hat{z}, 0) = 0, \tag{42}$$

where $c_{TL}(t_1) = c_{BL}(\tilde{t})$ and $c_{TR}(t_1) = c_{BR}(\tilde{t})$. The solution of (42) is given by

$$c_0(\hat{z}, t_1) = \int_0^{t_1} \sum_{n=1}^{\infty} (-1)^{n-1}(2n-1)\pi \exp\left(-(2n-1)^2 \frac{\pi^2}{4} s\right) \cos\left((2n-1)\frac{\pi}{2}\hat{z}\right)$$
$$\frac{(c_{TR}(t_1 - s) + c_{TL}(t_1 - s))}{2} \mathrm{d}s + \int_0^{t_1} \sum_{n=1}^{\infty} (-1)^n n\pi \exp\left(-n^2\pi^2 s\right) \sin\left(n\pi\hat{z}\right) (c_{TR}(t_1 - s)$$
$$- c_{TL}(t_1 - s))\mathrm{d}s. \tag{43}$$

A representative example of the solution when $\beta_H - \beta = o(1)$ is described in Subsection 5.2.

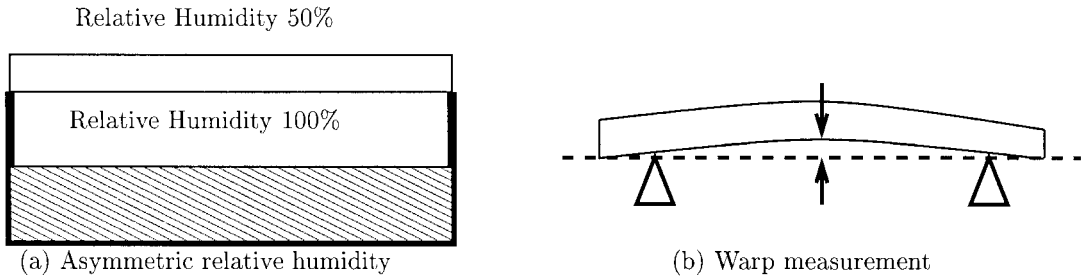

Figure 3. A schematic representation of the experimental set-up. The shaded region is water at 23 °C. Experiments take place in a climate room where the temperature is maintained at 23 °C throughout. The centre of the panel warps down in (a).

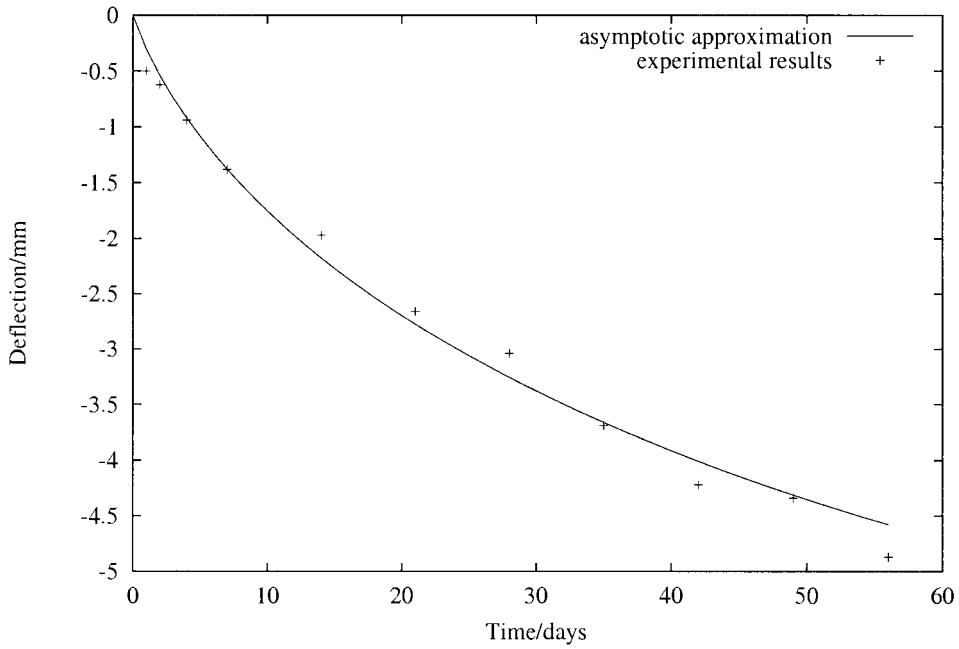

Figure 4. Comparison of the first term in the asymptotic expansion and experimental measurements (courtesy of TRESPA International BV) for the moisture induced warp of a panel with décor at $x = 23$cm.

5. Results

5.1. Experimental validation

5.1.1. *Measurement of panel warp*

We now outline the experimental measurement of panel warp. A test sample is placed over a container filled with water (as shown in Figure 3a). The container with test sample is then stored in a climate room with a relative humidity of 50% and a temperature of 23 °C. In this way the test sample is exposed to an asymmetric environment of 50% relative humidity on the top side and 100% on the bottom side (with the centre of the panel being displaced down in Figure 3a). At regular time intervals the warp of the test sample is measured. The panel is placed symmetrically on two fixed supports in order to perform the measurements. The panel warp is then measured in the middle of the two supports as the deviation from the plane

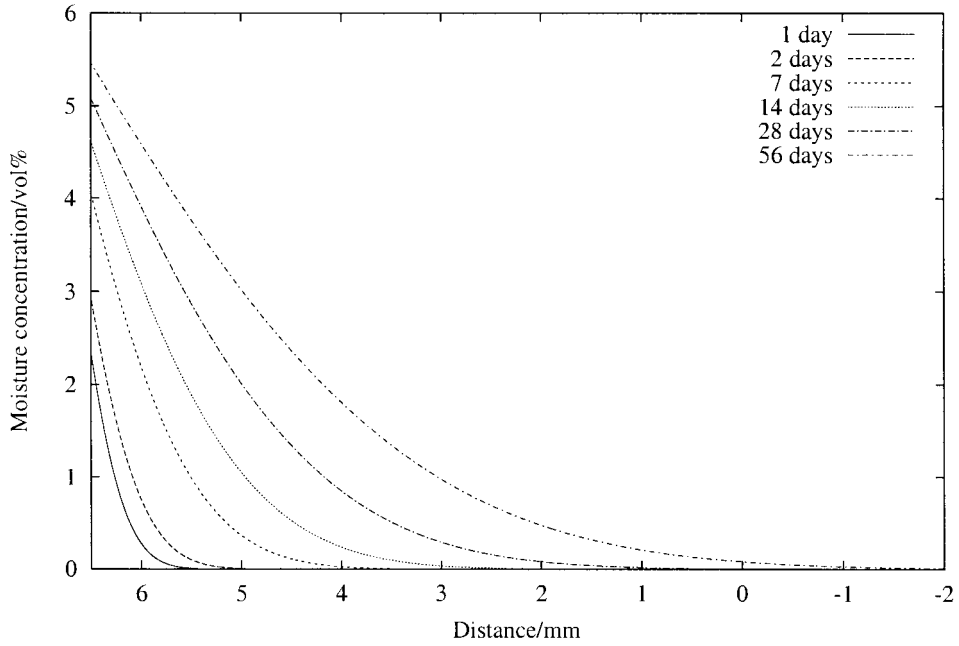

Figure 5. The first term in the asymptotic expansion for moisture concentration in a panel with décor. The surface at $z = 6{\cdot}5$mm is exposed to a relative humidity of 6·5vol%. The interval $-6.5\text{mm} < z < -2\text{mm}$ is not shown as the moisture concentrations are indistinguishable from zero.

containing the two support points (see Figure 3b). Experimental observations are shown in Figure 4.

The moisture uptake corresponding to a given relative humidity is required as a boundary condition to the moisture transport model (discussed below). In order to assess the moisture uptake at 50% and 100% relative humidity (and 23 °C), test samples were stored in a climate room over long time periods. The moisture uptake was measured after a steady state had been attained. The swelling was also recorded at various relative humidities in the range 50%..100% in a similar manner and found to be a linear function of the equilibrium moisture uptake.

5.1.2. *Moisture transport in a climate room*

We again adopt assumptions (i) and (ii) of Section 4 and we assume the temperature is constant. We also assume that the concentration of water $c(z, t)$ starts at a given constant level c_{init}, a constant concentration c_{init} is applied at the lower side and a constant concentration c_U at the upper side. The governing equation is the diffusion equation

$$\frac{\partial c}{\partial t} = \frac{\partial}{\partial z}\left(D\frac{\partial c}{\partial z}\right),$$

where D is the (constant) diffusion coefficient. A Robin boundary condition is required at $z = h$ and $z = -h$, namely

$$D\frac{\partial c}{\partial z}(h, t) = H(c_U - c(h, t)), \qquad D\frac{\partial c}{\partial z}(-h, t) = H(c(-h, t) - c_{\text{init}}),$$

where H is the (constant) mass-transfer coefficient. The initial condition is $c(z, 0) = c_{\text{init}}$. We now transform to dimensionless variables via $z = h\hat{z}$, $t = \tau\hat{t}$ and $c = c_{\text{init}} + (c_U - c_{\text{init}})\bar{c}$. The problem becomes

non-dimensional

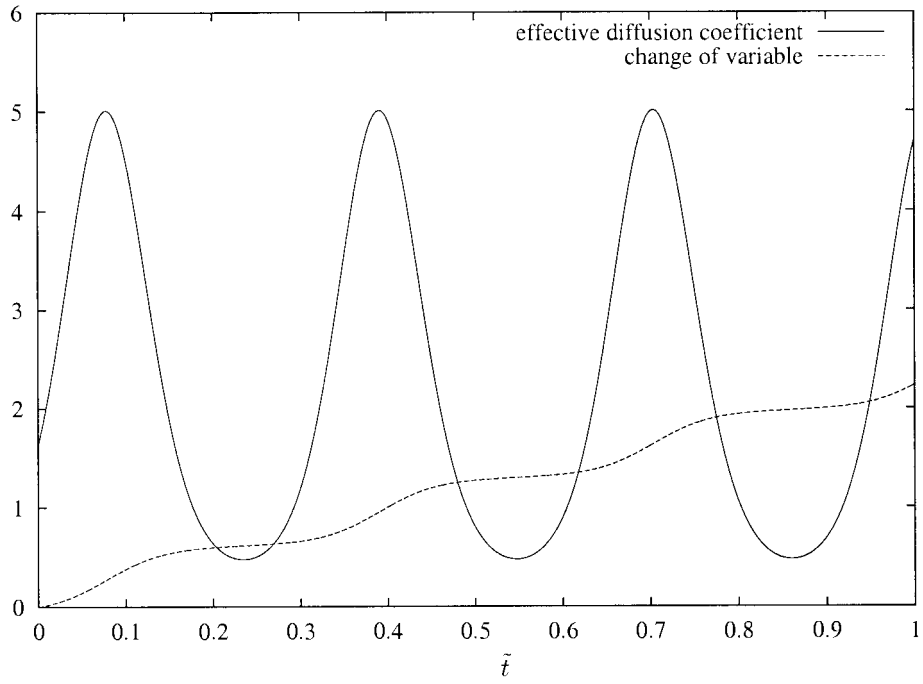

Figure 6. The effective moisture diffusion coefficient $\langle 1 \rangle$ and change of variable t_1 as a function of $\tilde{t}$.

$$\frac{\partial \bar{c}}{\partial \hat{t}} = \epsilon^2 \frac{\partial^2 \bar{c}}{\partial \hat{z}^2},$$

with the boundary conditions

$$K \frac{\partial \bar{c}}{\partial \hat{z}}(1, \hat{t}) = (1 - \bar{c}(1, \hat{t})), \qquad K \frac{\partial \bar{c}}{\partial \hat{z}}(-1, \hat{t}) = \bar{c}(-1, \hat{t}),$$

and initial condition $\bar{c}(\hat{z}, 0) = 0$. The constant $\epsilon^2 = D\tau/h^2$ is characteristic of the moisture diffusion length-scale $((D\tau)^{1/2})$ in time τ and $K = D/hH$. Typically, the parameter ϵ is small for the short time-scales of a few days in which we are primarily interested. The solution now depends on the order of magnitude of K. If $K = O(1)$ then the problem is self-similar and a uniformly valid approximation (in dimensional form) is given by (see [7, Section 2.8])

$$c \sim c_{\text{init}} + (c_U - c_{\text{init}}) H \left[\frac{-(h-z)}{D} \operatorname{erfc}\left(\frac{h-z}{2(Dt)^{1/2}} \right) + 2\sqrt{\frac{t}{\pi D}} \exp\left(\frac{-(h-z)^2}{4Dt} \right) \right] \quad (44)$$

as $\epsilon \to 0$,

however, if $K = O(\epsilon)$, then we obtain

$$c \sim c_{\text{init}} + (c_U - c_{\text{init}}) \left[-\exp\left(\frac{H(h-z)}{D} \right) \exp\left(\frac{H^2 t}{D} \right) \operatorname{erfc}\left(\frac{H\sqrt{t}}{\sqrt{D}} + \frac{(h-z)}{2\sqrt{Dt}} \right) + \operatorname{erfc}\left(\frac{h-z}{2\sqrt{Dt}} \right) \right] \quad \text{as} \quad \epsilon \to 0. \quad (45)$$

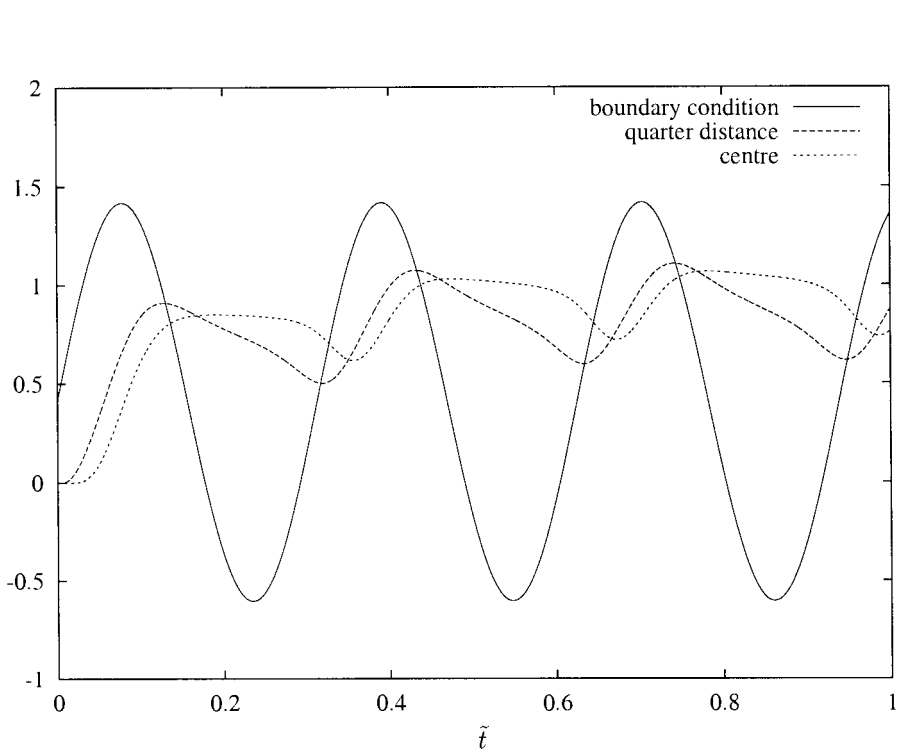

Figure 7. The leading-order moisture uptake at the boundary $c_{BL}(\tilde{t})$, at a quarter distance $c_0(\pm 0{\cdot}5, \tilde{t})$ and at the centre $c_0(0, \tilde{t})$ as a function of $\tilde{t}$.

The solution (44) may be derived from (45) in the limit $K \to \infty$.

The mass-transfer coefficient H may be determined from the experimental measurements of the panel warp by a least-squares fit. In general, the moisture concentration itself is difficult to measure with experiments. The concentration of moisture in a panel obtained from (45) is shown in Figure 5 for times varying from a few days to two months.

5.1.3. *Discussion*

The panel warp calculated with (31) is shown in Figure 4 corresponding to the moisture concentration in Equation (45). The agreement with experimental results is reasonable even for time periods longer than a few weeks when the solution for moisture concentration is at the limit of its range of validity. We note that the solution (29)–(31) is also limited to the small deformations of linear elasticity.

5.2. AN EXTERIOR APPLICATION

We now consider an example of an exterior application with $\beta = \beta_H$. The arbitrary functions in Section 4 are assumed to be of the form $c_L^*(t^*, \tilde{t}) = c_R^*(t^*, \tilde{t}) = \sin(t^*) + \sin(r\tilde{t})$ for the ambient moisture concentration, $T_L^*(t^*, \tilde{t}) = T_R^*(t^*, \tilde{t}) = \sin(t^*) + \sin(r\tilde{t})$ for the ambient temperature and $S^*(t^*, \tilde{t}) = \sin(t^*)(1 + \sin(r\tilde{t}))$ for the absorbed thermal radiation; r being defined in Table 2. Rather than computing (43), it is simpler from a numerical viewpoint to solve (42) directly with finite differences. The effective moisture diffusion coefficient and corresponding change of variables to t_1 (see (41)) are shown in Figure 6. As expected the effective

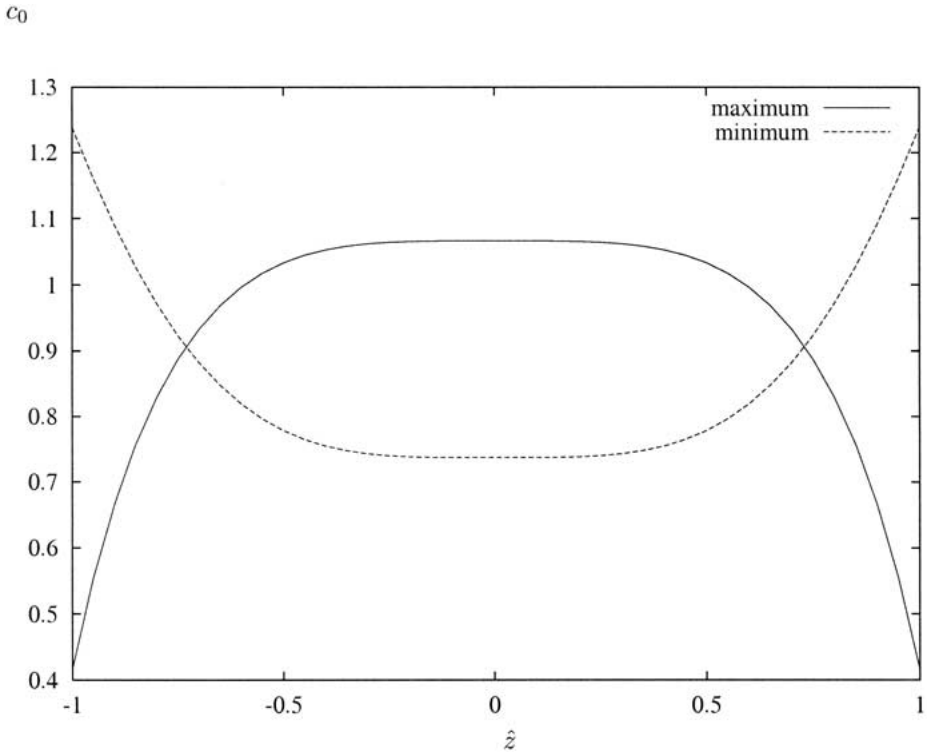

Figure 8. The leading-order moisture uptake as a function of $\hat{z}$ at two different times. The two times correspond to the maximum and the minimum of $c_0(0, \tilde{t})$ in the periodic steady state.

moisture diffusion coefficient is largest in summer and smallest in winter. The summer values of ambient concentration will therefore have much larger influence on the moisture uptake than the winter values. The moisture uptake at $\hat{z} = \pm 1$, $\hat{z} = \pm 0{\cdot}5$ and $\hat{z} = 0$ as a function of $\tilde{t}$ are shown in Figure 7. We see that there is an initial transient of approximately one year before the periodic steady state is attained. The maximum and minimum in the periodic steady state at $\hat{z} = \pm 0{\cdot}5$ lags $\hat{z} = \pm 1$ and similarly $\hat{z} = 0$ lags $\hat{z} = \pm 0{\cdot}5$ by a significant time. We therefore expect the shrinkage and swelling to lag in a similar manner. The leading-order moisture uptake as a function of $\hat{z}$ at two times corresponding to the maximum and minimum of $c_0(0, \tilde{t})$ are shown in Figure 8.

6. Concluding remarks

This paper has established a model for a material which swells by different amounts in the coordinate directions in response to moisture variations. This property is a result of the natural-fibre content and the manufacturing process. The material is anisotropic. However, we have modelled any anisotropy in the elastic properties as negligible. This approximation is justified by comparison with experimental results. The response to an increase in moisture concentration may be viewed as an anisotropic forcing term on an isotropic elastic body.

The moisture diffusion time-scale is four years, but warp has been observed a few days after manufacture. This apparent paradox has been explained by the discovery that the deflection of the centre plane of the panel is proportional to the moment of the moisture concentra-

tion. Therefore, small amounts of moisture adjacent to the surface of the panel have greater significance.

In exterior applications, the diffusion of moisture in the panel is complicated by temperature and moisture variations in the surrounding atmosphere. Once a panel is installed, there is an initial transient of approximately one year before a periodic steady state is attained. The periodic steady state is characterised by the moisture concentration in the panel (and therefore the swelling) lagging the atmospheric conditions. The maximum swelling of exterior panels will be observed several weeks after the most humid day of the year.

Acknowledgement

The authors thank P. Vriens for bringing this problem to their attention at the 36th European Study Group with Industry. Financial support for this work was provided by the TMR contract entitled ‘Differential Equations in Industry and Commerce’.

References

1. O. Suchland, Y. G. Feng, and D. P. Xu. The hygroscopic warping of laminated panels. *Forest Prod. J.* 45 (1995) 57–63.
2. S. P. Timoshenko and J. N. Goodier, *Theory of Elasticity*. New York: McGraw-Hill (1982) 567 pp.
3. A. E. H. Love, *A Treatise on the Mathematical Theory of Elasticity.* Cambridge: Cambridge University Press (1927) 643 pp.
4. P. V. Kaprielian, T. G. Rogers, and A. J. M. Spencer, Theory of laminated elastic plates. I. isotropic laminae. *Phil. Trans. R. Soc. London A 324* (1988) 565–594.
5. K. O. Friedrichs and R. F. Dressler, A boundary-layer theory for elastic plates. *Comm. Pure Appl. Math.* 14 (1961) 1–33.
6. D. Chandra, H. J. J. Gramberg, T. Ivashkova, W. R. Smith, A. Suryanto, J. H. M. ten Thije Boonkkamp, T. Ulicevic, and J. C. J. Verhoeven, Modelling of moisture induced warp in panels containing wood fibres. In: *Proceedings of the Thirty-sixth European Study Group with Industry,* 2000.
7. H. S. Carslaw and J. C. Jaeger, *Conduction of Heat in Solids*. Oxford: Clarendon Press (1959) 510 pp.